J Mater Sci (2010) 45:4256–4264
DOI 10.1007/s10853-009-4128-x

EUROMAT 2009

Fundamental issues of reactive wetting by liquid metals

O. Dezellus · N. Eustathopoulos

Received: 14 November 2009 / Accepted: 12 December 2009 / Published online: 8 January 2010

Abstract After a brief presentation of thermodynamics and kinetics of non-reactive wetting, the recent results and theoretical developments concerning the reactive wetting of solids by liquid metals are reviewed. A section is devoted to illustrate and discuss the effect of interfacial reactions in removing the wetting barriers existing on many ceramic and metallic solids.

Introduction

This review concerns the wetting of high-temperature solids, mainly ceramics, by liquid metals and alloys. Many metal/ceramic couples are far from equilibrium and the resulting interfacial reactions can strongly modify the chemistry, structure and topography of the contact area. These changes affect both the spreading kinetics and the ultimate degree of wetting and those aspects of reactive wetting that can be exploited in practice to control wetting and adhesion are reviewed in this article.

The article is organized in three parts. The main features of non-reactive wetting of metals on various types of solids are rapidly presented in "Non-reactive wetting" section. "Reactive wetting" section describes, the main part of the article, thermodynamics and kinetics of reactive wetting. After briefly describing the basic aspects of the "Reaction product control" model, recent results and developments of this model are given in more detail. "Interfacial reactions" section is dealt with the role of interfacial reactions in the removal of wetting barriers existing on many metallic and ceramic solids, and illustrated with several examples.

O. Dezellus (✉)
LMI - UMR CNRS 5615, University Lyon 1, 43 Bd du 11 Novembre 1918, 69100 Villeurbanne, France
e-mail: olivier.dezellus@univ-lyon1.fr

N. Eustathopoulos
SIMaP – UMR CNRS 5615, INP – Grenoble, 1130 rue de la Piscine, 38042 St Martin d'Hères, France

Non-reactive wetting

Thermodynamics

As a general rule, the interaction energy between a liquid and a solid substrates is quantified by the work of adhesion W_a related to the characteristic surface energies σ_{ij} of the solid (S)–liquid (L)–vapour (V) system by the Dupré equation:

$$W_a = \sigma_{SV} + \sigma_{LV} - \sigma_{SL} \quad (1)$$

Combining this expression with Young's equation $\cos\theta = \frac{\sigma_{SV}-\sigma_{SL}}{\sigma_{LV}}$ leads to the following fundamental equation of wetting, known as the Young–Dupré equation:

$$\cos\theta = \frac{W_a}{\sigma_{LV}} - 1 \quad (2)$$

This equation shows that the equilibrium contact angle obtained for a given liquid metal on a solid substrate results from the competition of two types of forces: adhesion forces that develop between the liquid and solid phases, expressed by W_a (tending to increase the common area thus improving wetting), and cohesion forces of the liquid taken into account by the surface energy of the liquid σ_{LV} acting in the opposite direction (the cohesion energy of the liquid is roughly equal to $2\sigma_{LV}$). Liquid metals are high cohesion energy liquids—indeed their cohesion energy at melting point represents more than 90% of the cohesion energy of the same metal in the solid state. Thus, according to the

Young–Dupré equation, good wetting of a liquid metal on a solid substrate, i.e. a cos θ close to unity, can be obtained only if the work of adhesion is also high, which is possible if the interfacial bond is strong, i.e. chemical.

For this reason, good wetting is the general rule for liquid metals on solid metals whatever the intensity of interaction between liquid and solid, the interfacial bond being metallic, i.e. strong (see Table 1). Liquid metals also wet semi-conductors such as Si, Ge or SiC [26, 30, 35], because the cohesion of semi-conductors has a metallic character near the free surface. Finally, liquid metals also wet ceramics such as carbides, nitrides or borides of transition metals, because a significant part of the cohesion of these materials is provided by metallic bonds [11, 39]. Solids that are not wetted by non-reactive liquid metals include the different forms of carbon [6], iono-covalent oxides and covalent ceramics with a high band gap such as BN or AlN [25, 27].

It should be emphasized that, even with wettable solids, contact angle values less than 90° can be prevented by the presence of wetting barriers on the solid surface. Thus, many of the ceramics with a partially metallic character (such as borides of transition metals), some covalent ceramics (such as SiC and Si_3N_4) and many metallic solids (stainless steels, superalloys, Al containing alloys and so on), are also easily oxidized and their wettability by non-reactive metals is strongly affected by oxide films that may be very tenacious, especially at low temperatures [11, 31, 33].

Spreading kinetics

In non-reactive systems, the spreading rate is controlled by the viscous flow and described by a power function of the triple line velocity U versus the instantaneous contact angle θ

$$U \sim \theta^n \tag{3a}$$

For a spherical shaped drop with a base radius R, $U = \mathrm{d}R/\mathrm{d}t$, and Eq. 3a leads to

$$R^{3n+1} \sim t \tag{3b}$$

De Gennes [4] has developed an analytical approach in which the spreading rate is considered to be limited by the viscous dissipation in the drop bulk leading to $n = 3$, whereas Blake's model, which is based on dissipation at atomic level at the triple line, leads to $n = 2$ [1]. Because the viscosity of molten metals is very low, the spreading time (i.e. the time needed for millimetric size droplets to reach capillary equilibrium) is less than 10^{-1} s in the case of non-reactive systems with equilibrium contact angle values higher than 20° [26, 30, 37, 43]. A significantly longer spreading time was observed in [21] for a couple with an equilibrium contact angle very close to zero.

Reactive wetting

In 1996, Landry and Eustathopoulo [22] proposed a model to describe wetting for metal/ceramic systems in which the interfacial reactions lead to the formation of continuous layers of a new compound. According to the model ('reaction product control' model), both the final contact angle and the spreading kinetics are governed by the interfacial reaction. Note that in 2000, Saiz et al. [36] suggested that reactive wetting is caused mainly by adsorption, whereas spreading kinetics is controlled by the migration of a ridge formed at the solid–liquid–vapour triple line. In [13], a detailed analysis of existing experimental data was published that did not confirm Saiz et al.'s approach. Since that date no new results or new developments concerning this approach have been published and for this reason Saiz et al.'s approach is not reported in this review.

Reactive versus non-reactive wetting

Recently, Bougiouri et al. [2] illustrated the first-order transition, from the point of view of wetting, that is associated with the non-reactive to reactive transition in the case of Ni–Si alloys on vitreous carbon (C_V) substrates: when the silicon content in the liquid alloy is below the minimum silicon content needed for SiC formation (35 at.% at 1200 °C), no SiC is formed at the liquid/solid interface and the system is characterized by a high contact angle value (123°). Conversely, when the Si content exceeds the reactivity limit, a thin continuous SiC layer is formed along the whole interface, leading to spreading of the liquid alloy. The continuous layer is revealed for example by the triple line receding during cooling after capillary equilibrium is reached (see Fig. 1).

Moreover, the authors compared the work of immersion ($W_i = \sigma_{SL} - \sigma_{SV} = -\sigma_{LV} \cdot \cos\theta$) obtained with the same Ni–Si alloys either in the reactive case on carbon or in the non-reactive case on SiC substrates (see Fig. 2). It appears clearly that both values, on C and SiC substrates, lie on the

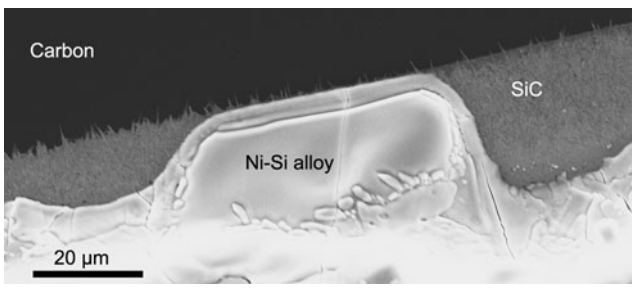

Fig. 1 SEM image of a triple line region of a Ni–66.8 at.%Si alloy on C_v observed from above. X-ray micro-analysis of area exposed after receding reveals the presence of C and Si only [2]

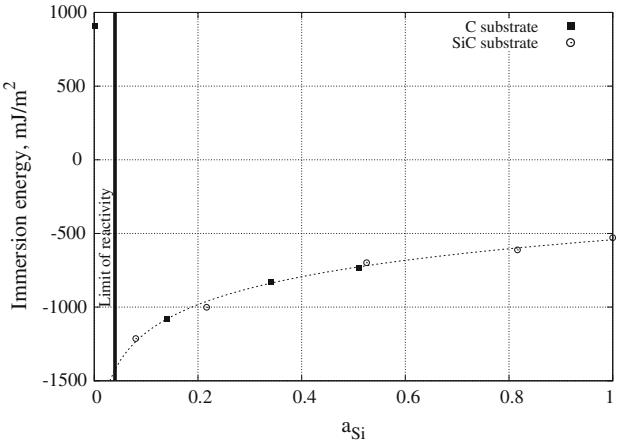

Fig. 2 Immersion energy $W_i = \sigma_{SL} - \sigma_{SV}$ versus Si activity of NiSi alloys on C_v (*squares*, [2]) and on SiC (*circles*, [34]). $T = 1200$ °C. The reactivity limit for the C_v substrate is shown by the *dotted line*

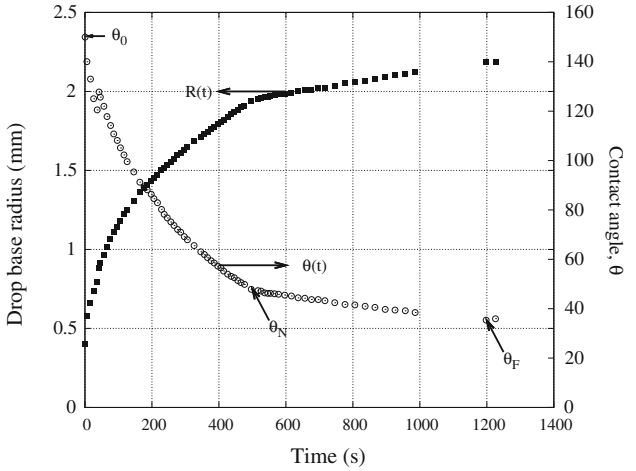

Fig. 3 Typical change in drop base radius R and contact angle θ with time in the case of reactive spreading kinetics limited by the local process at the triple line. Ni–63 at.%Si alloy on vitreous carbon at 1200 °C [2]

same curve. This quantitative agreement clearly indicates that the non-wetting to wetting transition observed between non-reactive and reactive alloys is due to the replacement of vitreous carbon by wettable SiC at the interface.

Spreading kinetics

The spreading time observed for reactive metal/ceramic systems, where a new compound is formed at the interface during spreading, is in the range 10^1–10^4 s, i.e. several orders of magnitude higher than for non-reactive systems. As a consequence, the spreading rate in reactive systems is not limited by viscous dissipation but by the rate of interfacial reaction at the triple line [22]. In turn, this rate is controlled by the slower of two successive phenomena that take place in the reaction process: diffusive transport of reacting species to or from the triple line and local reaction kinetics at the triple line.

Control by the local reaction at the triple line

In the case of control by the local reaction at the triple line, the rate of reaction and hence the triple line velocity are expected to be constant with time [22]. Since the first experimental evidence obtained for unalloyed aluminium on carbon [22], constant or nearly constant triple line velocities U have been observed for different systems such as the CuSi/C [7] and NiSi/C [2] systems, for CuSi alloys on oxidized SiC [10], for pure Si on oxidized Si_3N_4 [12] and for Ti-containing Ni-based alloys on AlN [19]. Figure 3 shows an example of a NiSi alloy on vitreous carbon. After transient spreading, where the contact angle decreases in a few tens of seconds from 160° to 110°, the spreading rate dR/dt continues to decrease but only slightly ('quasi-linear spreading') and tends towards a constant value U^* when θ tends towards θ_N. The quasi-linear spreading proves that the spreading rate is not limited by long-range diffusion of the reactive element (Si), but by the local reaction process at the triple line. At $\theta = \theta_N$, a second wetting stage appears abruptly, accompanied by a net decrease in spreading rate. This stage is discussed later.

For the quasi-linear stage, a model leading to analytical expressions of contact angle as a function of time has been developed [7, 8]. Assuming that, at any time, the instantaneous contact angle θ reflects the local chemistry of the interface at the triple line (referred to hereafter as TL) where the interface is composite, partly of the liquid/initial substrate type and partly of the liquid/reaction product type. Moreover, the reaction rate is assumed to be controlled by the dissolution process, i.e. by the process of atom transfer occurring at the substrate/alloy interface.

The following equations describing spreading were derived for the change in contact angle with time t:

$$\cos\theta_F - \cos\theta = (\cos\theta_F - \cos\theta_0)\cdot\exp(-k\cdot t) \qquad (4)$$

And for the dependence of the spreading rate U on the instantaneous contact angle θ:

$$\frac{U}{F(\theta)} = k\cdot\left(\frac{3V}{\pi}\right)^{1/3}\cdot(\cos\theta_F - \cos\theta) \qquad (5)$$

with $F(\theta) = -\frac{\cos\theta\cdot\left(2-3\cdot\cos\theta+\cos^3\theta\right)-\sin^4\theta}{\sin\theta\cdot(2-3\cdot\cos\theta+\cos^3\theta)^{4/3}}$ and V being the volume of the liquid droplet.

The constant k in Eqs. 4 and 5 is proportional to the kinetic constant k_d and to the driving force $\Delta\mu$ of the dissolution process. For the NiSi/C system, $\Delta\mu$ is the difference between the chemical potential of carbon in the solid

and the liquid and is related to the activity of Si in the alloy a_{Si} by Eq. 6:

$$\Delta\mu = RT \cdot \ln \frac{a_{Si}}{a_{Si}^{I}} \quad (6)$$

where a_{Si}^{I} is the minimum value of Si activity for SiC formation by reaction between Si in the alloy and solid carbon (a_{Si}^{I} corresponds to the equilibrium of three phases: initial substrate, reaction product and liquid).

According to this expression, logarithmic plots of cos θ_F cos θ versus time would be linear with a slope equal to $-k$. An example is given in Fig. 4 for Ni–63 at.%Si alloy on vitreous carbon at different temperatures. The experimental data agree with the linearity predictions in a wide domain of theta. The sharp change in the slope of straight lines reflects the high value of the activation energy of the dissolution process (about 250 kJ/mol in this case) [2]. For dissolution reactions controlled by the atomic process at the interface, the kinetic constant k_d is in principle sensitive to the crystallographic structure of the initial substrate. This is confirmed by the strong variation in the TL velocities observed for Cu–50 at.%Si on two different types of carbon: vitreous carbon and pseudo-monocrystalline graphite (Fig. 5).

As for the influence of the activity of reactive element on spreading kinetics, according to Eq. 6, this would be weak, in agreement with experimental findings [3]. According to Eq. 5, plots of the spreading rate U divided by $F(\theta)$ versus the cosine of the instantaneous contact angle would be linear. This was verified by the results of Muolo et al. [24] for the CuAg–5 at.%Ti alloy on three different substrates, two oxidic (an alumina–zirconia ceramic and zirconia stabilized by yttria) and one metallic (the superalloy Inconel 738).

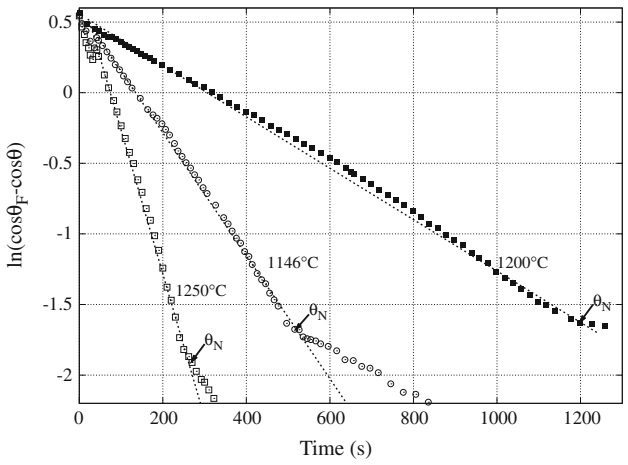

Fig. 4 Natural logarithm of cos θ_F − cos θ versus time t for Ni–63 at.%Si alloy/C_v system at different temperatures [7]

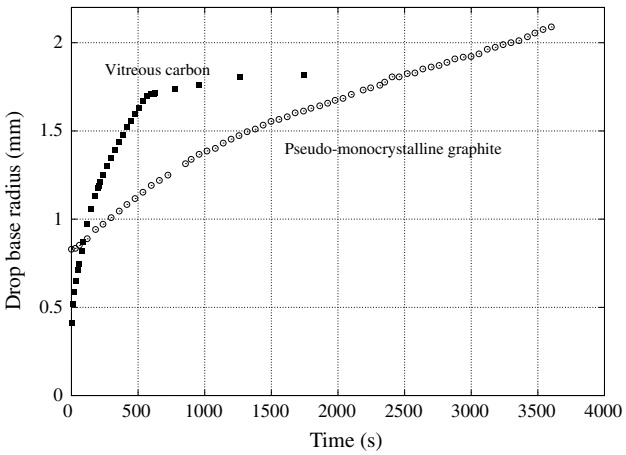

Fig. 5 Change in drop base radius versus time t for Cu–50 at.%Si alloy on two different types of carbon: vitreous carbon and pseudo-monocrystalline graphite at 1200 °C [5]

Control by local reaction at the TL: strong versus weak coupling

Figure 3 shows that the spreading rate changes abruptly at a contact angle noted θ_N. As discussed in detail elsewhere [5], this reflects the change in the microscopic configuration at TL. At $t < t_N$ ($\theta > \theta_N$), direct contact between the liquid and the initial substrate results in a high dissolution rate and in a strong coupling between the local chemical reaction and the spreading kinetics. The microstructure of the reaction product in this stage is columnar [3, 7] At $t > t_N$, the liquid no longer has direct access to the initial substrate surface and a slow reaction takes place by nucleation and growth of reaction product particles occurring on the substrate free surface *in front of TL* (see Fig. 6 for schematic description of TL configuration). Direct experimental evidence for this mechanism, which leads to formation of an equiaxial microstructure, was given recently in [3] (see Fig. 7). Table 1 reports the main features of the two wetting stages. The last column gives the growth rate of the reaction layer on the carbon-free surface once the capillary equilibrium was attained (in this case the reaction front advances while TL does not move). The comparison indicates that the rate of the linear spreading stage is much closer to the growth rate of silicon carbide during the decoupled growth than to the TL velocity in the quasi-linear stage.

Diffusion-controlled reactive wetting

Diffusion-controlled wetting was modelled by Mortensen et al. [23] in 1997. According to this model, the rate of isothermal spreading U = dR/dt is time dependent and varies in direct proportion to the instantaneous contact angle θ:

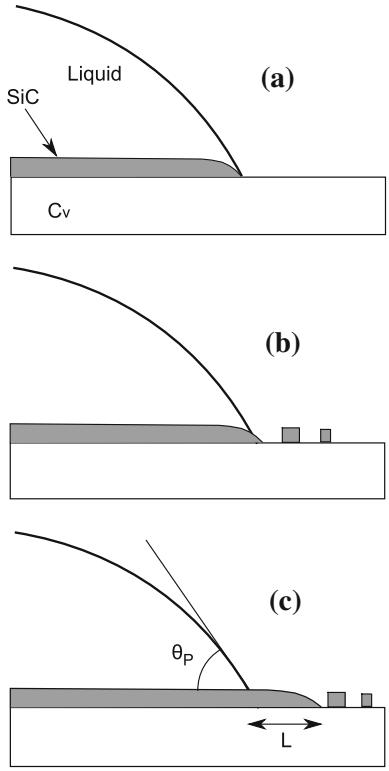

Fig. 6 Schematic representation of the configuration at the triple line. **a** At $\theta > \theta_N$, direct contact between the liquid and initial substrate leads to strong coupling between the local chemical reaction and spreading kinetics. **b** At $\theta < \theta_N$, the liquid no longer has direct access to the initial substrate surface and coupling is weak. **c** When θ_P is reached, decoupled growth of reaction product ahead of TL occurs (according to [5])

$$\frac{dR}{dt} = \frac{2 \cdot D \cdot F(t)}{e \cdot n_v} \cdot (C_0 - C_e) \cdot \theta \quad (7)$$

where D is the diffusion coefficient in the liquid, n_v the number of moles of reactive solute per unit volume of the reaction product, e the reaction product thickness at the TL, C_0 the nominal (far-field) drop reactive solute concentration and C_e the concentration of reactive solute in equilibrium with the reaction product (such that $C = C_e$ at the TL). $F(t)$ is strictly a function of time but in fact varies so little that it can be taken to be constant, remaining close to 0.04 in usual sessile drop experiments [23].

When compared with experimental results, this relation shows good agreement for systems such as AgCuSn–Ti/C_v [9], in which the final contact angle is close to zero. However, some discrepancies remain in other cases such as Cu–Cr/C_v. For this system, the intercept of the line giving dR/dt versus θ with the θ-axis is not at the origin ($\theta = 0$), but rather at a finite angle close to 40° [38] as shown in Fig. 8. Note that the Mortensen equation was established by assuming that all solute flux is consumed by the reaction at the TL, thus neglecting any thickening of the reaction layer behind the TL. However, this assumption is hardly verified in the Cu–Cr/C_v system, where chromium carbide interfacial reaction layers are relatively thick (several micrometers) and continue to thicken if the drop is held at

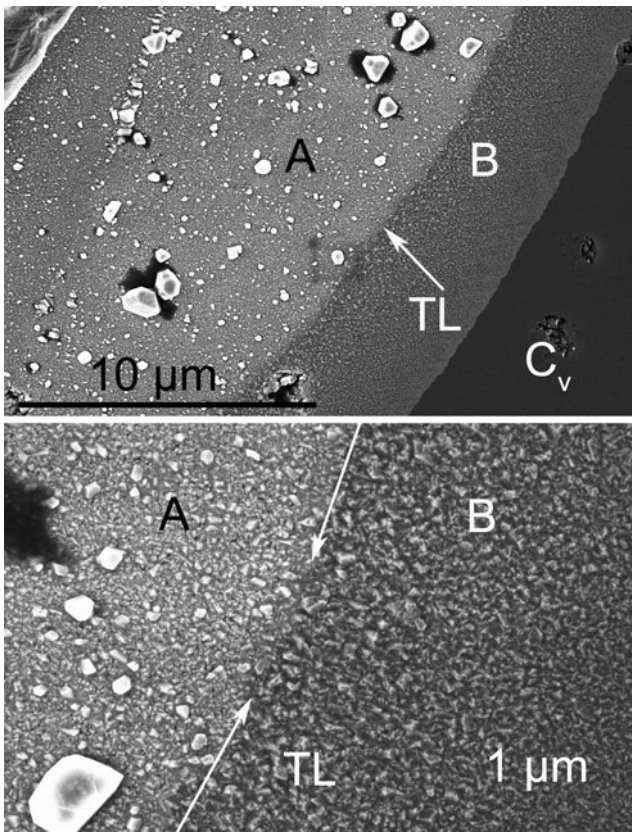

Fig. 7 Top view of the reaction layers close to the triple line for Al–25 at.%Si/C_v. Zone A (observed after removing, by dissolution, the Al–Si alloy) corresponds to SiC formed during weakly coupled spreading ($\theta_P < \theta < \theta_N$), whereas zone B corresponds to the growth of a film ahead of the TL after capillary equilibrium is reached ($\theta = \theta_P$) [3]

Table 1 Wetting by non-reactive liquid metals

Type of solid	Wetting	Examples
Solid metals	$\theta \ll 90°$	Pb/Fe—40° [29, 31]
		AgCu/stainless steel—10°–60° [20]
Semi-conductors		Sn/Ge—40° [26]
		Ag/SiC—33°–65° [35]
Ceramics with a partially metallic character		AgCu/Ti_3SiC_2—10° [11]
		Au/ZrB_2—25° [39]
Carbon materials	$\theta \gg 90°$	Au/C—119°–135° [6]
Iono-covalent oxides		Cu/Al_2O_3, Cu/$Si0_2$—120°–130° [14]
Covalent ceramics		Au/AlN—134°–138° [27]
		Au/BN—135°–150° [25]

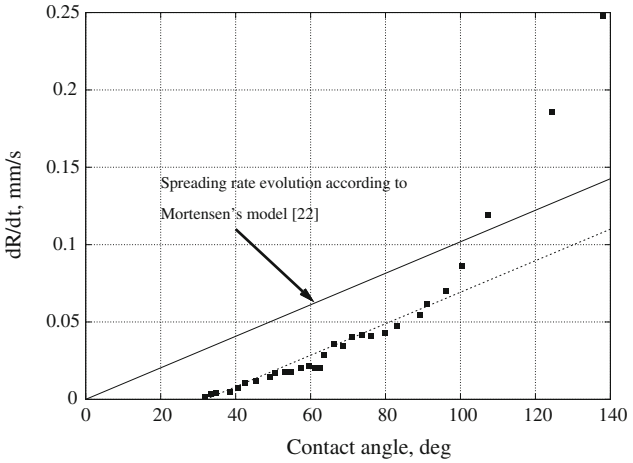

Fig. 8 Experimental triple line velocity as a function of instantaneous contact angle θ for Cu–1 at.%Cr on vitreous carbon at 1150 °C [38] and spreading rate according to Mortensen's model [23]

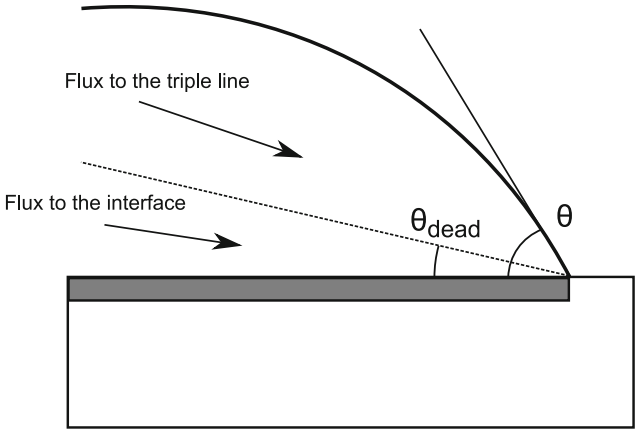

Fig. 9 Schematic representation of the physical meaning of the dead angle that must be subtracted from θ in Mortensen's analytical solution (Eq. 7). The flux across the solid angle delimited by the 'dead angle' is deviated away from the TL and consumed in thickening of the reaction layer behind the TL

temperature, indicating rapid carbide growth kinetics in this system.

To verify the effect of thickening on the spreading kinetics, numerical calculations of the wetting process by finite-element modelling was recently performed in the case of Cu–Cr alloy on C_v [16]. Calculations were performed by arbitrarily varying the value of the diffusion coefficient D_C of C in chromium carbide. It was found that for very low values of D_C the rate of reaction product growth behind the TL is negligible. The TL velocity is then simply proportional to the instantaneous contact angle θ, as predicted by Mortensen's analytical model. When D_C increases, the curve giving the TL velocity U as a function of θ remains linear, retaining the same slope, but is shifted so that its intercept with the θ-axis increases progressively. Finally, the experimental data are relatively well predicted for D_C equal to 6×10^{15} m^2/s which is a realistic value for this system.

As a conclusion, the simulation yields the following general result: interfacial reactivity manifests itself by the presence of a finite 'dead-angle' that must be subtracted from θ in Mortensen's analytical solution, this equation remaining otherwise essentially valid. The physical meaning of the dead angle is presented in Fig. 9: the flux across the solid angle delimited by the 'dead angle' is deviated away from the TL and consumed in thickening of the reaction layer behind the TL.

Interfacial reactions versus wetting barriers

Most of the non-oxide ceramics are easily oxidized and the oxide films on their surface act as wetting barriers, leading to non-wetting by non-reactive liquid metals. Reactivity at liquid/solid interfaces can remove these wetting barriers thus improving wetting. Symmetrically, reactivity can also lead to the formation of a reaction product less wetted than the initial substrate, i.e. to the formation of a wetting barrier.

Table 2 Wetting of vitreous carbon by Cu–50 at.%Si at $T = 1200$ °C

Regime	$\theta > \theta_N$	$\theta_P < \theta < \theta_N$	$\theta = \theta_P$
$R(t)$ law	Quasi-linear	Linear	–
U (nm/s)	630[a]	54[a]	20[b]
Activation energy (kJ/mol)	255 ± 30	335 ± 15	–
Microstructure	Columnar	Equiaxial	Equiaxial

Characteristics of the three different regimes [5]

[a] At $\theta = \theta_N$

[b] Average value, $L = 30$ μm, $\Delta t = 1500$ s

An interesting example was given by Frage et al. [15] in the Au–TiC system. The authors showed that pure Au does not wet TiC the contact angle being about 130°, a value that is similar to that obtained for Au on carbon substrates (see Table 2). Because of the strong interaction between Au and Ti, slight dissolution of Ti from the substrate into the liquid occurs. However, as the solubility of C in Au is much smaller than that of Ti, graphite precipitates at the interface leading to a contact angle of 130°, which is a characteristic of Au on graphite (Table 2). A similar case where reactivity leads to the formation of a wetting barrier was already reported by Kalogeropoulou et al. [17] in the Ag/SiC system where dissolution of Si in the melt leads to a precipitation of graphite at the liquid/solid interface. As for the Au/TiC system, Frage et al. performed some additional experiments with Au containing different alloying

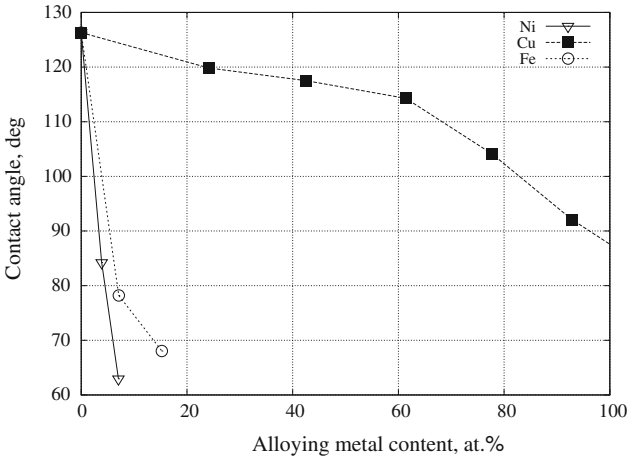

Fig. 10 Contact angle between stoichiometric TiC and Au alloys at 1150 °C [15]

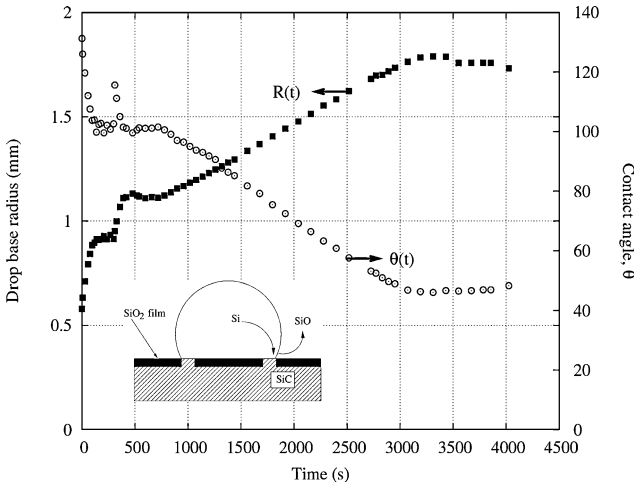

Fig. 11 Time-dependent variation in drop base radius R and contact angle θ for Cu–40 at.%Si on the C face of an α-SiC single crystal covered by a silica layer 60–70 nm thick [10]

elements. The solubility of C in molten Ni being several orders of magnitude higher than in Au, small Ni additions increase the solubility of C significantly, thereby preventing the formation of the graphite layer on the TiC substrate. In this case, the experimental results show a dramatic decrease in contact angle towards values in the range 60°–80° for 3–7 at.%Ni (see Fig. 10) without any reaction product at the interface. In this system, the action of Ni is to remove the wetting barrier by dissolution.

Silicon carbide is a typical example of non-oxide ceramic that is easily oxidized. Indeed even under high vacuum SiC, surfaces at temperatures less than 1100 °C are usually covered by a silica film that acts as a wetting barrier. However, with alloys containing Si, the removal of silica is possible by the formation of the volatile suboxide SiO by reaction between silicon and silica at the TL. Dezellus et al. [10] performed a dedicated study with CuSi alloys on silicon carbide substrates which had been deliberately oxidized to obtain oxide films a few tens of nanometres thick. A typical wetting experiment consists of two steps (see Fig. 11): (1) Firstly, fast spreading is observed towards 100°, the equilibrium contact angle value of Cu–Si alloy on bulk silica. Then, the contact angle remains constant during a time that depends on the initial silica film thickness. During this first step, deoxidation occurs close to the TL, because in this particular area the distance between the liquid/solid interface (where the dissolution of silica takes place) and the liquid/vapour interface (where SiO evaporation occurs) is the smallest. (2) As soon as the liquid comes into contact with the true SiC surface, spreading occurs and the contact angle decreases towards the equilibrium contact angle on SiC. This second step is characterized by a constant TL velocity and corresponds to reactive spreading limited by the kinetics of the dissolution reaction of the silica layer at the TL. Note that when large pieces of SiC are brazed with Me–Si alloys, the deoxidation mechanism of the SiC surface by SiO formation gives the geometrical configuration, a crucial role in alloy wetting, the difficulty increasing in the order: sessile drop → 'capillary' brazing → 'sandwich' brazing [18].

At low temperatures, normal metallic solids are covered by thin oxide films, a few nanometres thick, formed rapidly in contact with air at room temperature. Such oxides, that may be stable even in high vacuum or in low partial pressure of oxygen gas mixtures, are not wetted by liquid metals [14, 20, 31, 32]. Wetting can be strongly improved by reactions where intermetallic compounds are formed, leading to the replacement, in situ, of the oxidized surface by a clean surface of an intermetallic compound [32] (see Fig. 12). For this reason, as a general rule, the final degree of wetting in liquid metal/solid metal systems in which intense reactions occur at the interface is much less sensitive to environmental factors than in non-reactive systems.

Conclusions

Interfacial reactions leading to the formation of continuous layers of a new compound can improve wetting or conversely worsen it. This depends on the wettability by the liquid metal of the new compound compared to the wettability of the initial solid substrate. In some cases, interfacial reactions can also improve wetting by removing wetting barriers (mainly oxide films) existing on otherwise wettable substrates surface. As for spreading kinetics in reactive metal/ceramic systems, a significant improvement in understanding and modelling this process has been achieved over the last 10 years. Thus, an analytical model

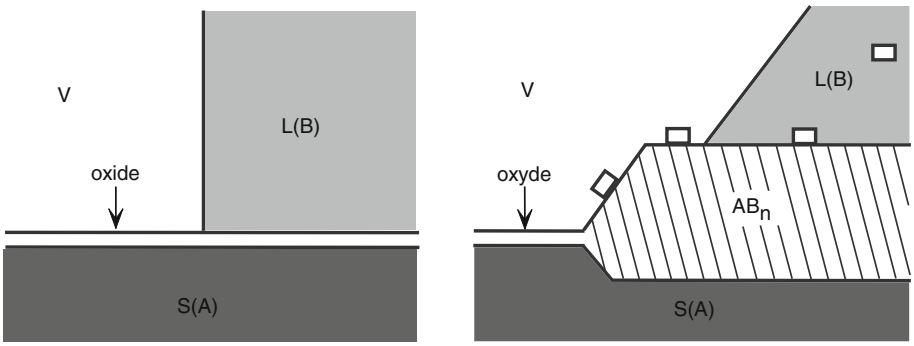

Fig. 12 Schematic description of the region close to the triple line for an oxidized metal **a** in the case of a non-reactive liquid metal B-solid metal A couple and **b** in the case of formation of a layer of intermetallic compound AB_n at the interface [32]

was developed to describe spreading kinetics in systems with control by local reaction kinetics at the TL. Moreover, the model proposed by Mortensen et al. for diffusion-controlled reactive spreading was improved to take into account the influence on spreading rate of the reaction occurring at the interface behind the TL.

This review does not report on 'dissolutive wetting'. This is wetting accompanied by dissolution of the solid into the liquid with formation of a macroscopically non-planar solid/liquid interface [14, 40]. Dissolutive wetting is a common process in liquid metal/solid metal systems but it is also relevant in some metal/ceramic systems such as Ni/C [14], Ni/HfB_2 [28] and AuNi/ZrB_2 [39]. Although recent studies performed with model liquid metal/solid metal couples have contributed significantly to improving our knowledge of dissolutive wetting [21, 30, 40–42], more work is needed to obtain a satisfactory description of the thermodynamics and kinetics of this type of wetting.

References

1. Blake TD (1993) Wettability. Marcel Dekker, New York, pp 251–310
2. Bougiouri V, Voytovych R, Dezellus O, Eustathopoulos N (2007) J Mater Sci 42(6):2016. doi:10.1007/s10853-006-1483-8
3. Calderon N, Voytovych R, Narciso J, Eustathopoulos N (in press) J Mater Sci. doi:10.1007/s10853-009-3909-6
4. de Gennes PG (1985) Rev Mod Phys 57(3):827
5. Dezellus O (2000) Contribution à l'étude des mécanismes de mouillage réactif. PhD thesis, INP-Grenoble, France
6. Dezellus O, Eustathopoulos N (1999) Scr Mater 40(11):1283
7. Dezellus O, Hodaj F, Eustathopoulos N (2002) Acta Mater 50:4741
8. Dezellus O, Hodaj F, Eustathopoulos N (2003) J Eur Ceram Soc 23(15):2797
9. Dezellus O, Hodaj F, Mortensen A, Eustathopoulos N (2001) Scr Mater 44:2543
10. Dezellus O, Hodaj F, Rado C, Barbier JN, Eustathopoulos N (2002) Acta Mater 50:979
11. Dezellus O, Voytovych R, Li A, Constantin G, Bosselet F, Viala J (in press) J Mater Sci. doi:10.1007/s10853-009-3941-6
12. Drevet B, Voytovych R, Israel R, Eustathopoulos N (2009) J Eur Ceram Soc 29(11):2363
13. Eustathopoulos N (2005) Curr Opin Solid State Mater Sci 9(4–5):152
14. Eustathopoulos N, Nicholas MG, Drevet B (1999) Wettability at high temperatures. Pergamon materials series, vol 3. Pergamon, Oxford
15. Frage N, Froumin N, Dariel MP (2002) Acta Mater 50(2):237
16. Hodaj F, Dezellus O, Barbier JN, Mortensen A, Eustathopoulos N (2007) J Mater Sci 42(19):8071. doi:10.1007/s10853-007-1915-0
17. Kalogeropoulou S, Rado C, Eustathopoulos N (1999) Scr Mater 41(7):723
18. Koltsov A, Hodaj F, Eustathopoulos N (2008) Mater Sci Eng A 495(1–2):259
19. Koltsov A, Dumont M, Hodaj F, Eustathopoulos N (2006) Mater Sci Eng A 415(1–2):171
20. Kozlova O, Voytovych R, Devismes M-F, Eustathopoulos N (2008) Mater Sci Eng A 495(1–2):96
21. Kozlova O, Voytovych R, Protsenko P, Eustathopoulos N (in press) J Mater Sci. doi:10.1007/s10853-009-3924-7
22. Landry K, Eustathopoulos N (1996) Acta Mater 44(10):3923
23. Mortensen A, Drevet B, Eustathopoulos N (1997) Scr Mater 36(6):645
24. Muolo ML, Ferrera E, Morbelli L, Passerone A (2004) Scr Mater 50(3):325
25. Naidich YV (1981) Progress in surface and membrane sciences, vol 14. Academic Press, New York, pp 353–484
26. Naidich YuV, Zabuga VV, Perevertailo VM (1992) Adgeziya Rasplavov i Paika Materialov 27:23
27. Naidich YV, Taranets NY (1995) In: Eustathopoulos N (ed) Proceedings of the international conference on high temperature capillarity. Reproprint, Bratislava, p 138
28. Passerone A, Muolo ML, Valenza F, Monteverde F, Sobczak N (2009) Acta Mater 57(2):356
29. Popel SI, Kozhurkov VN, Zaharova TV (1971) Zashchita Metall 7:421
30. Protsenko P, Kozlova O, Voytovych R, Eustathopoulos N (2008) J Mater Sci 43(16):5669. doi:10.1007/s10853-008-2814-8
31. Protsenko P, Terlain A, Jeymond M, Eustathopoulos N (2002) J Nucl Mater 307–311(Part 2):1396
32. Protsenko P, Terlain A, Traskine V, Eustathopoulos N (2001) Scr Mater 45(12):1439
33. Rado C, Eustathopoulos N (2004) Interface Sci 12(1):85
34. Rado C, Kalogeropoulou S, Eustathopoulos N (1999) Acta Mater 47(2):461
35. Rado C, Kalogeropoulou S, Eustathopoulos N (2000) Mater Sci Eng A 276(1–2):195
36. Saiz E, Cannon RM, Tomsia AP (2000) Acta Mater 48 (18–19):4449
37. Saiz E, Tomsia AP (2004) Nat Mater 3(12):903
38. Voitovitch R, Mortensen A, Hodaj F, Eustathopoulos N (1999) Acta Mater 47(4):1117

39. Voytovych R, Koltsov A, Hodaj F, Eustathopoulos N (2007) Acta Mater 55(18):6316
40. Warren JA, Boettinger WJ, Roosen AR (1998) Acta Mater 46(9):3247
41. Yin L, Meschter SJ, Singler TJ (2004) Acta Mater 52(10):2873
42. Yin L, Murray BT, Singler TJ (2008) Acta Mater 54(13):3561
43. Zaidi M (2008) PhD thesis, Ecole Centrale de Paris, France